Engineering Analysis with Boundary Elements ▮ (▮▮▮▮) ▮▮▮–▮▮▮

Contents lists available at ScienceDirect

Engineering Analysis with Boundary Elements

journal homepage: www.elsevier.com/locate/enganabound

Applications of the modified Trefftz method for the Laplace equation

Yung-Wei Chen [a,*], Chein-Shan Liu [b], Jiang-Ren Chang [a]

[a] Department of Systems Engineering and Naval Architecture, National Taiwan Ocean University, Keelung 20224, Taiwan, ROC
[b] Department of Mechanical and Mechatronic Engineering, National Taiwan Ocean University, Keelung 20224, Taiwan, ROC

ARTICLE INFO

Article history:
Received 25 September 2007
Accepted 30 May 2008

Keywords:
Laplace equation
Artificial circle
DtR mapping
Modified Trefftz method
Mixed-boundary value problem
Singular problem

ABSTRACT

In this paper, the Laplace problems are solved by using the modified Trefftz method. For discontinuous boundary problem, singular problem, and degenerate scale problem, the conventional Trefftz method encounters the numerical instability owing to rank deficiency and high-order T-complete functions. To overcome these problems, the characteristic length of problem domain and high-order T-complete functions is introduced to obtain a modified Trefftz method, equipping with a characteristic length factor to make sure that this method is stable. Besides, the high-order T-complete functions can be clearly described for the discontinuous boundary conditions. Comparing with the solutions in the previous literature, the present method is powerful even for the problem with complex boundary and with adding random noise on the boundary data. It is also successfully solving the degenerate scale problem, resulting to a highly accurate result never seen before.

1. Introduction

After 1980, the most widely used numerical methods for engineering applications are the finite difference method, finite element method, and boundary element method (BEM). Especially, the BEM has become quite popular in recent years due to its advantage of the reduction of dimensionality. Only several years ago, the meshless methods started to capture the interest of the researchers in the community of computational mechanics because those methods are meshes free and only boundary nodes are necessary [1–4]. Among those meshless methods, the Trefftz method is a boundary-type solution procedure using only the T-complete functions satisfying the governing equation. It was the first proposed in 1926 by Trefftz [5]. The mathematical theory of the Trefftz method has been studied by Herrera et al. [6]. The Trefftz method includes a direct and an indirect formulation [7]. In the direct formulation, the weighted residual expression is derived from the differential equation by using the T-complete functions as the weight functions. In the indirect formulation, the solution is approximated by a superposition of T-complete functions with unknown coefficients, which are determined to satisfy the boundary conditions. Recently, the Trefftz method has a broad application in engineering computations, for example, Berardi et al. [8], Kita et al. [9], Lu et al. [10], and Portela et al. [11].

Although the Trefftz method has much relevant research, it still has some drawbacks for hindering its successful development such as in the discontinuous boundary problems, singular problems and degenerate scale problems. Generally, in order to overcome these difficulties to obtain a regularized solution one usually used the truncated singular value decomposition together with the regularization parameter determined by the L-curve method. Li et al. [12] have given a complete comparison of the Trefftz, collocation and other boundary methods. They concluded that collocation Trefftz method (CTM) is the simplest algorithm and provides the most accurate solution with the best numerical stability. However, the conventional CTM may exists a major drawback that the resulting linear equations system is seriously ill-conditioned. In order to obtain an accurate solution of the linear equations the above-mentioned special techniques cannot be avoided which in turns lead to a complex solution process.

In order to overcome these difficulties appeared in conventional CTM, Liu [13–15] proposed a modified Trefftz method, refined this method by taking the characteristic length into the T-complete functions, such that the condition number of the resulting linear equations system can be greatly reduced. Nevertheless, this method got easily instable solutions such as for degenerate scale problems and singular problems, while utilizing the low-order T-complete functions. For the above-mentioned problems, we are going to compare the maximum errors under different characteristic lengths and elements number, and the best accuracy by using high-order T-complete functions can be obtained.

This paper is organized as follows. In Section 2, we derive the first kind Fredholm integral equation along a given artificial circle.

* Corresponding author. Tel.: +886 2 24622192x6017; fax: +886 2 24625945.
E-mail address: d93510004@mail.ntou.edu.tw (Y.-W. Chen).

0955-7997/$ - see front matter © 2008 Elsevier Ltd. All rights reserved.
doi:10.1016/j.enganabound.2008.05.008

In Section 3, we consider a collocation method to find the Fourier coefficients. In Section 4, we use some examples, including the Motz problem and torsion problem, to compare with the results appeared in the previous literature. Finally, in Section 5, we summarize the conclusions.

2. Basic formulations

In this paper, we consider new methods to solve the mixed-boundary value problem, which consists of the Laplace equation and the mixed-boundary condition specified on a non-circular boundary:

$$\begin{aligned} &\Delta u = u_{rr} + \frac{1}{r}u_r + \frac{1}{r^2}u_{\theta\theta} = 0, \\ &r<\rho \quad \text{or} \quad r>\rho, \quad 0\leqslant\theta\leqslant 2\pi, \end{aligned} \tag{1}$$

$$\beta_D u(\rho,\theta) + \beta_N u_n(\rho,\theta) = h(\theta), \quad 0\leqslant\theta\leqslant 2\pi, \tag{2}$$

where $h(\theta)$ is a given function, and $\rho=\rho(\theta)$ is a given contour describing the boundary shape of the interior or exterior domain S. The contour Γ in the polar coordinates is given by $\Gamma=\{(r,\theta)|r=\rho(\theta),\ 0\leqslant\theta\leqslant 2\pi\}$, which is the boundary of the problem domain S. For exterior problem S is unbounded, while S is bounded for interior problem. On the other hand, in order to deal with the boundary condition conveniently, β_D and β_n satisfy $\beta_D^2+\beta_N^2>0$.

If the whole boundary is composed of the Dirichlet boundary condition, then we have $\beta_D=1$ and $\beta_N=0$. Conversely, if the whole boundary is composed of the Neumann boundary condition, then we have $\beta_D=0$ and $\beta_N=1$. Therefore, for a mixed-boundary condition with u prescribed on a partial boundary Γ_1 and with u_n prescribed on a partial boundary $\Gamma_2=\Gamma/\Gamma_1$, we have $\beta_D=1$ and $\beta_N=0$ on Γ_1 and $\beta_D=0$ and $\beta_N=1$ on Γ_2.

In the above, through some efforts, we can derive

$$u_n(\rho,\theta) = \frac{\partial u(\rho,\theta)}{\partial r} - \frac{\rho'}{\rho^2}\frac{\partial u(\rho,\theta)}{\partial\theta}, \tag{3}$$

where n is an outward-normal direction of the boundary.

We replace Eq. (2) by the following boundary condition:

$$u(R_0,\theta) = f(\theta), \quad 0\leqslant\theta\leqslant 2\pi, \tag{4}$$

where $f(\theta)$ is an unknown function to be determined, and R_0 is a given positive constant, such that the disk $D=\{(r,\theta)|r\leqslant R_0,\ 0\leqslant\theta\leqslant 2\pi\}$ can cover S for the interior problem, or it is inside in the complement of S, that is, $D\in R^2/\bar{S}$ for the exterior problem. Specifically, we may let

$$R_0\leqslant\rho_{\min}=\min_{\theta\in[0,2\pi]}\rho(\theta) \quad \text{(exterior problem)}, \tag{5}$$

$$R_0\geqslant\rho_{\max}=\max_{\theta\in[0,2\pi]}\rho(\theta) \quad \text{(interior problem)}. \tag{6}$$

Because R_0 is uniquely determined by the contour of the considered problem by Eq. (5) or Eq. (6); we do not worry how to choose R_0. In the later, it will be clear that R_0 specifies a characteristic length of the problem domain, and also plays a major role to control the stability of the numerical method.

The basic idea is to replace the original complicated Robin boundary condition in Eq. (2) on a complicated contour by a simpler boundary condition (4) on a specified circle. However, the price we should pay is that we require deriving a new equation to solve $f(\theta)$. If the task can be finished and if the function $f(\theta)$ is available, then the advantage of this replacement is that we have a Fourier series expansion of $u(r,\theta)$ satisfying Eqs. (1) and (4):

$$u(r,\theta) = a_0 + \sum_{k=1}^{\infty}\left[a_k\left(\frac{R_0}{r}\right)^{\pm k}\cos k\theta + b_k\left(\frac{R_0}{r}\right)^{\pm k}\sin k\theta\right], \tag{7}$$

where

$$a_0 = \frac{1}{2\pi}\int_0^{2\pi} f(\xi)\,\mathrm{d}\xi, \tag{8}$$

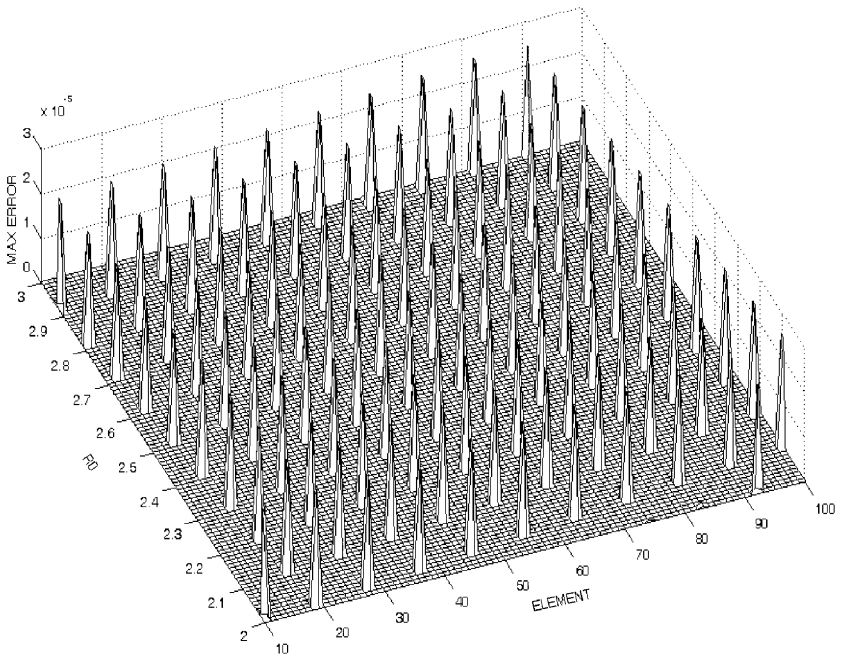

Fig. 1. The distribution of maximum errors under different characteristic lengths and elements.

Please cite this article as: Chen Y-W, et al. Applications of the modified Trefftz method for the Laplace equation. Eng Anal Bound Elem (2008), doi:10.1016/j.enganabound.2008.05.008

$$a_k = \frac{1}{\pi}\int_0^{2\pi} f(\xi)\cos k\xi \,\mathrm{d}\xi, \tag{9}$$

$$b_k = \frac{1}{\pi}\int_0^{2\pi} f(\xi)\sin k\xi \,\mathrm{d}\xi \tag{10}$$

are the Fourier coefficients of $f(\theta)$. In Eq. (7), the positive sign is used for the exterior problem, and conversely the minus sign is used for the interior problem.

From Eqs. (3) and (7), it follows that

$$u_n(\rho,\theta) = \sum_{k=1}^{\infty}\gamma^k\left[\left\{\mp\frac{ka_k}{\rho} - \frac{kb_k\rho'}{\rho^2}\right\}\cos k\theta + \left\{\frac{ka_k\rho'}{\rho^2} \mp \frac{kb_k}{\rho}\right\}\sin k\theta\right], \tag{11}$$

where

$$\gamma(\theta) := \left(\frac{R_0}{\rho(\theta)}\right)^{\pm 1}. \tag{12}$$

By imposing condition (2) on Eq. (7) and utilizing Eq. (11) we obtain

$$a_0\beta_D + \sum_{k=1}^{\infty}[a_kE^k(\theta) + b_kF^k(\theta)] = h(\theta), \tag{13}$$

where

$$E^k(\theta) := \gamma^k\left[\beta_D\cos k\theta \mp \beta_N\frac{k}{\rho}\cos k\theta + \beta_N\frac{k\rho'}{\rho^2}\sin k\theta\right], \tag{14}$$

$$F^k(\theta) := \gamma^k\left[\beta_D\sin k\theta \mp \beta_N\frac{k}{\rho}\sin k\theta - \beta_N\frac{k\rho'}{\rho^2}\cos k\theta\right]. \tag{15}$$

Substituting Eqs. (8)–(10) for a_0, a_k, and b_k into Eq. (13) leads to the first kind Fredholm integral equation:

$$\int_0^{2\pi} K(\theta,\xi)f(\xi)\,\mathrm{d}\xi = h(\theta), \tag{16}$$

where

$$K(\theta,\xi) = \frac{\beta_D}{\pi} + \frac{1}{\pi}\sum_{k=1}^{\infty}[E^k(\theta)\cos k\xi + F^k(\theta)\sin k\xi] \tag{17}$$

is a kernel function.

Eq. (16) is an exact boundary condition, providing a mapping from the Dirichlet boundary condition on a simple artificial circle to the Robin boundary condition on the original complicated boundary. This mapping is named the Dirichlet to Robin mapping, abbreviated as the DtR mapping. However, it is difficult to directly

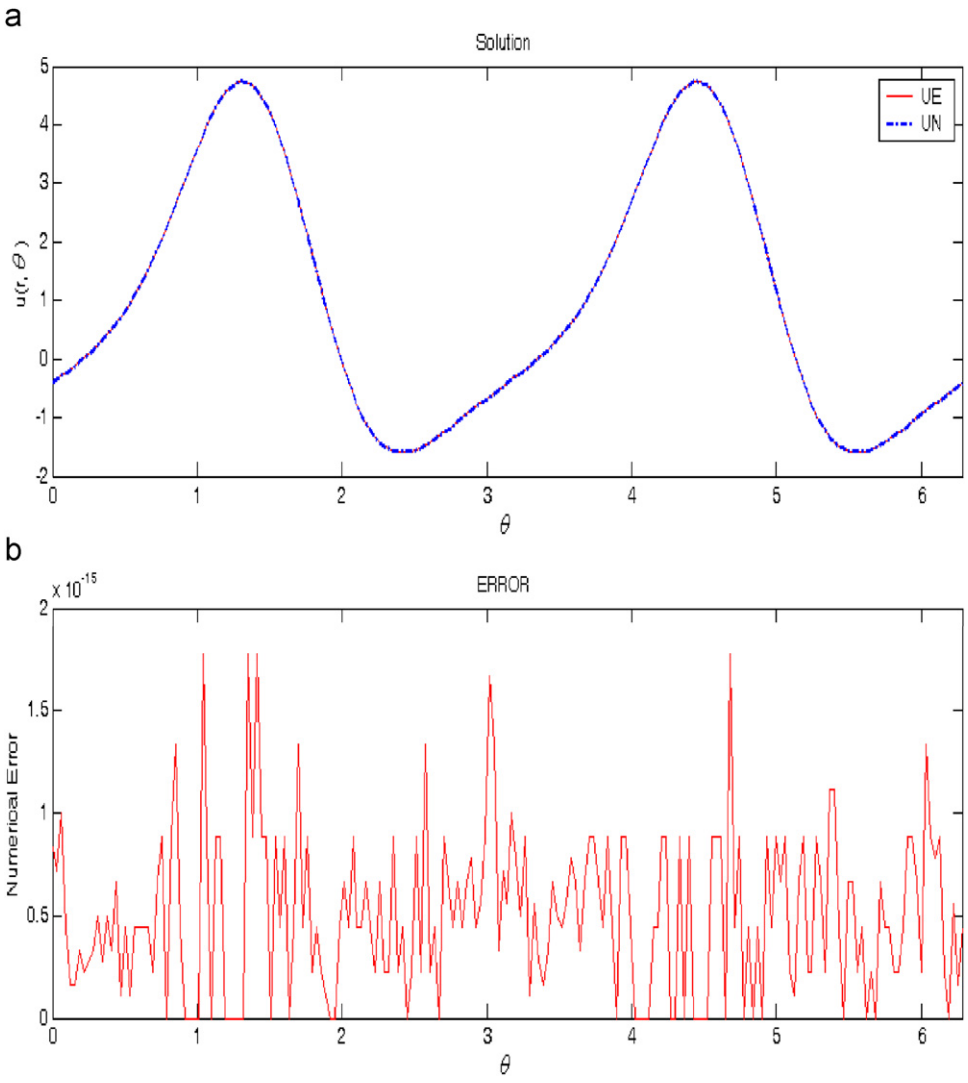

Fig. 2. Comparing the exact solution and numerical solution for Example 1 in (a), and the numerical error is plotted in (b).

Please cite this article as: Chen Y-W, et al. Applications of the modified Trefftz method for the Laplace equation. Eng Anal Bound Elem (2008), doi:10.1016/j.enganabound.2008.05.008

inverse Eq. (16) to obtain the exact boundary data $f(\theta)$. Liu [16] has applied the regularization integral equation method to solve Eq. (16) for the Dirichlet boundary value problems. But in this paper, we are going to directly solve Eq. (7) to obtain the Fourier coefficients as simple as possible.

3. The collocation method

We consider a mixed-boundary condition with u prescribed on a partial boundary Γ_1 and with u_n prescribed on the other boundary $\Gamma_2 = \Gamma/\Gamma_1$. Therefore, we have $\beta_D = 1$ and $\beta_N = 0$ on Γ_1, while $\beta_D = 0$ and $\beta_N = 1$ on Γ_2, i.e.,

$$u(\rho,\theta) = h_D(\theta) \quad (\rho,\theta) \in \Gamma_1, \tag{18}$$

$$u_n(\rho,\theta) = h_N(\theta) \quad (\rho,\theta) \in \Gamma_2. \tag{19}$$

The series expansions in Eqs. (7) and (11) are well suited to the entire solution domain. Hence, the admissible functions with finite terms can be used to determine the unknown coefficients a_k and b_k:

$$u(\rho,\theta) = a_0 + \sum_{k=1}^{m}[A_k a_k + B_k b_k], \tag{20}$$

$$u_n(\rho,\theta) = \sum_{k=1}^{m}[C_k a_k + D_k b_k], \tag{21}$$

where

$$A_k(\theta) := \gamma^k \cos(k\theta), \tag{22}$$

$$B_k(\theta) := \gamma^k \sin(k\theta), \tag{23}$$

$$C_k(\theta) := \mp\frac{k}{\rho}A_k + \frac{k\rho'}{\rho^2}B_k, \tag{24}$$

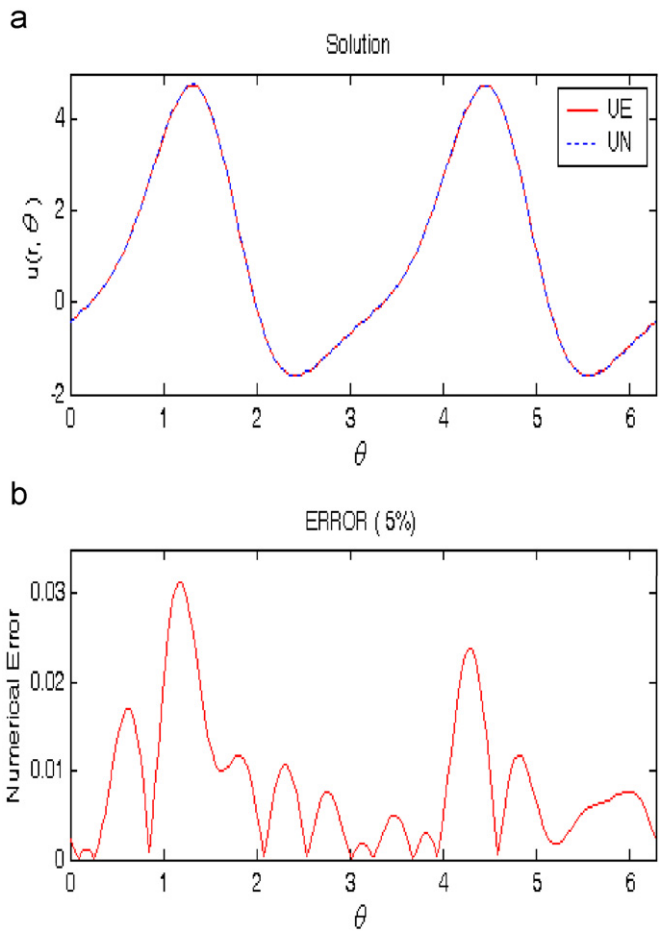

Fig. 4. Comparing the exact solution and numerical solution with 5% noise in the boundary data for Example 1 in (a), and the numerical errors are plotted in (b).

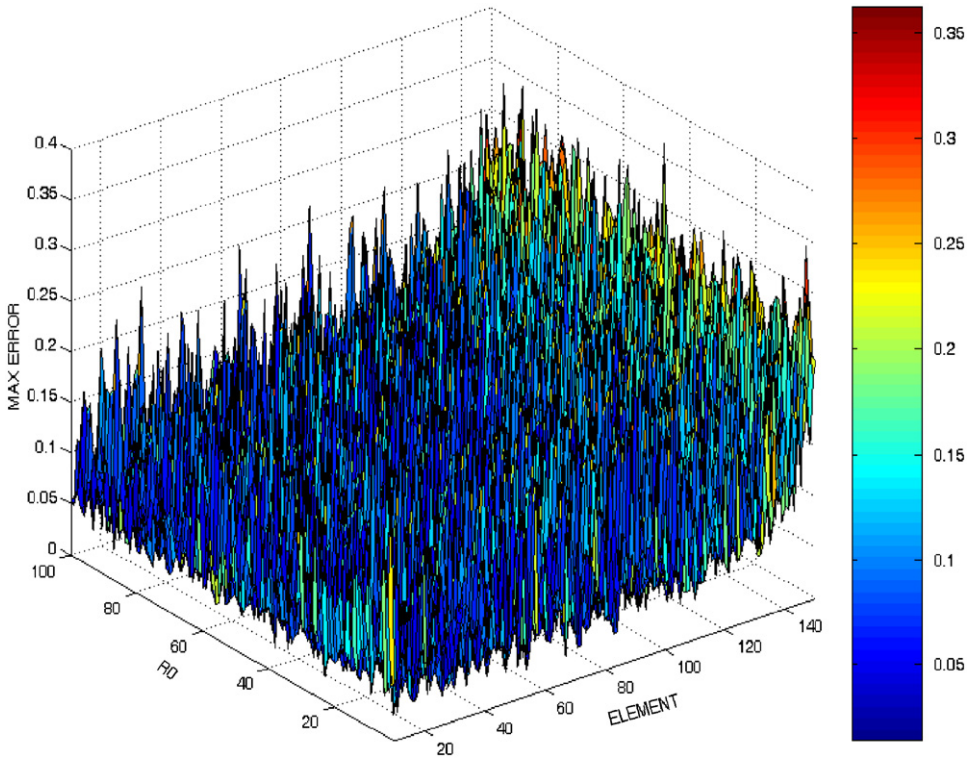

Fig. 3. The distribution of maximum errors under different characteristic lengths and elements, with 5% noise in the boundary data.

Please cite this article as: Chen Y-W, et al. Applications of the modified Trefftz method for the Laplace equation. Eng Anal Bound Elem (2008), doi:10.1016/j.enganabound.2008.05.008

$$D_k(\theta) := \mp\frac{k}{\rho}B_k - \frac{k\rho'}{\rho^2}A_k. \tag{25}$$

Here, we introduce the collocation method. Eqs. (20) and (21) are imposed at different collocation points on two different boundaries with $[\rho(\theta_i),\theta_i]\in\Gamma_1$ and $[\rho(\bar{\theta}_j),\bar{\theta}_j]\in\Gamma_2$,

$$a_0 + \sum_{k=1}^{m}[A_k(\theta_i)a_k + B_k(\theta_i)b_k] = h_D(\theta_i), \tag{26}$$

$$\sum_{k=1}^{m}[C_k(\bar{\theta}_j)a_k + D_k(\bar{\theta}_j)b_k] = h_N(\bar{\theta}_j). \tag{27}$$

When the indices i and j in Eqs. (26) and (27) run from 1 to m, we obtain a linear equations system with dimensions $n = 2m+1$:

$$\begin{bmatrix} 1 & A_1(\theta_0) & B_1(\theta_0) & \cdots & A_m(\theta_0) & B_m(\theta_0) \\ 1 & A_1(\theta_1) & B_1(\theta_1) & \cdots & A_m(\theta_1) & B_m(\theta_1) \\ 0 & C_1(\bar{\theta}_1) & D_1(\bar{\theta}_1) & \cdots & C_m(\bar{\theta}_1) & D_m(\bar{\theta}_1) \\ \vdots & \vdots & \vdots & \vdots & \vdots & \vdots \\ 1 & A_1(\theta_m) & B_1(\theta_m) & \cdots & A_m(\theta_m) & B_m(\theta_m) \\ 0 & C_1(\bar{\theta}_m) & D_1(\bar{\theta}_m) & \cdots & C_m(\bar{\theta}_m) & D_m(\bar{\theta}_m) \end{bmatrix} \begin{bmatrix} a_0 \\ a_1 \\ b_1 \\ \vdots \\ a_m \\ b_m \end{bmatrix} = \begin{bmatrix} h_D(\theta_0) \\ h_D(\theta_1) \\ h_N(\bar{\theta}_1) \\ \vdots \\ h_D(\theta_m) \\ h_N(\bar{\theta}_m) \end{bmatrix}. \tag{28}$$

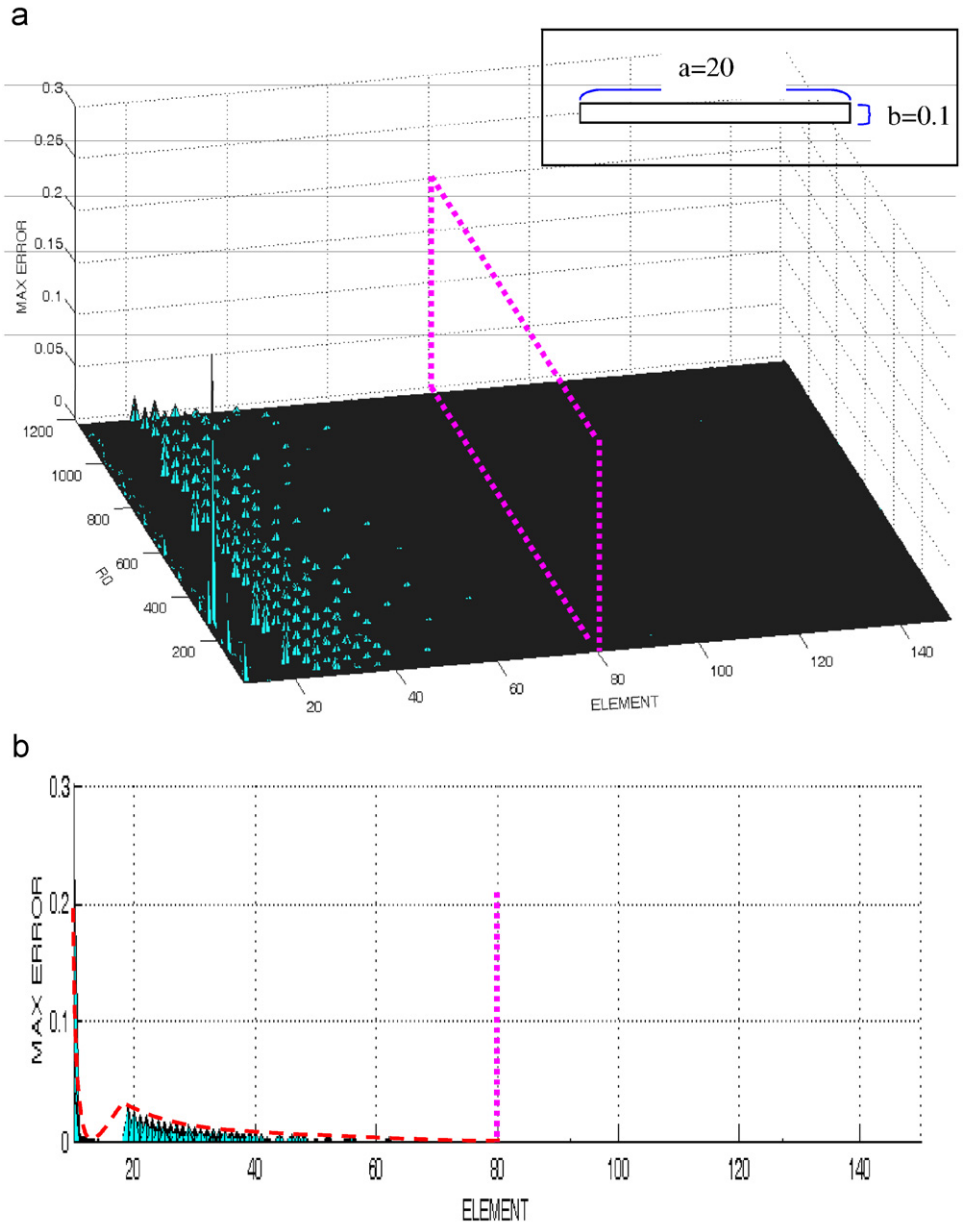

Fig. 5. The distribution of maximum errors under different characteristic lengths and elements in (a). In (b), we are plotting the convergent trend of the elements.

Please cite this article as: Chen Y-W, et al. Applications of the modified Trefftz method for the Laplace equation. Eng Anal Bound Elem (2008), doi:10.1016/j.enganabound.2008.05.008

In the above, θ_0 is an extra collocated point on the boundary Γ_1 used to supplement another equation to determine the unknowns.

We denote the above equation by

$$Rc = b_1, \tag{29}$$

where $c = [a_0,\ a_1,\ b_1,\ldots,a_m,\ b_m]^{\mathrm{T}}$ is the vector of unknown coefficients. The conjugate gradient method can be used to solve the following normal equation:

$$Ac = b, \tag{30}$$

where

$$A := R^{\mathrm{T}}R, \quad b := R^{\mathrm{T}}b_1. \tag{31}$$

Inserting the calculated c into Eq. (7) we thus have a semi-analytical solution of

$$u(r,\theta) = c_1 + \sum_{k=1}^{\infty}\left[c_{2k}\left(\frac{R_0}{r}\right)^{\pm k}\cos k\theta + c_{2k+1}\left(\frac{R_0}{r}\right)^{\pm k}\sin k\theta\right] \tag{32}$$

where $(c_1,\ldots,c_{2m+1})$ are the component of c.

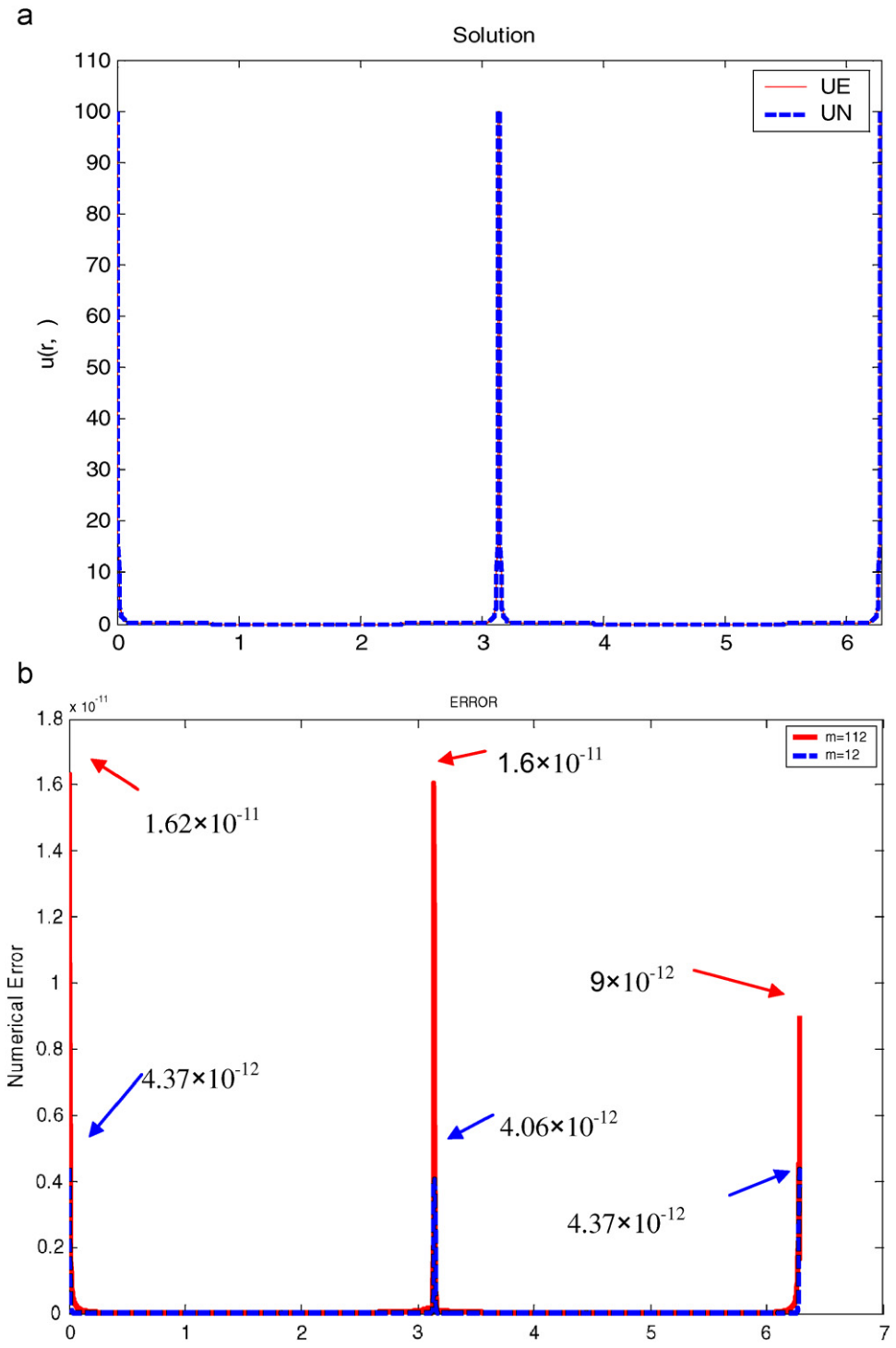

Fig. 6. Comparing the exact solution and numerical solution for Example 2 in (a) and the numerical errors are plotted in (b).

Please cite this article as: Chen Y-W, et al. Applications of the modified Trefftz method for the Laplace equation. Eng Anal Bound Elem (2008), doi:10.1016/j.enganabound.2008.05.008

4. Numerical tests

In order to test the stability of the modified Trefftz method when the boundary data are contaminated by random noise, which is investigated by adding the different levels of random noise on the boundary data. We use the function RANDOM_NUMBER given in Fortran to generate the noisy data $R(i)$, where $R(i)$ are random numbers in $[-1, 1]$.

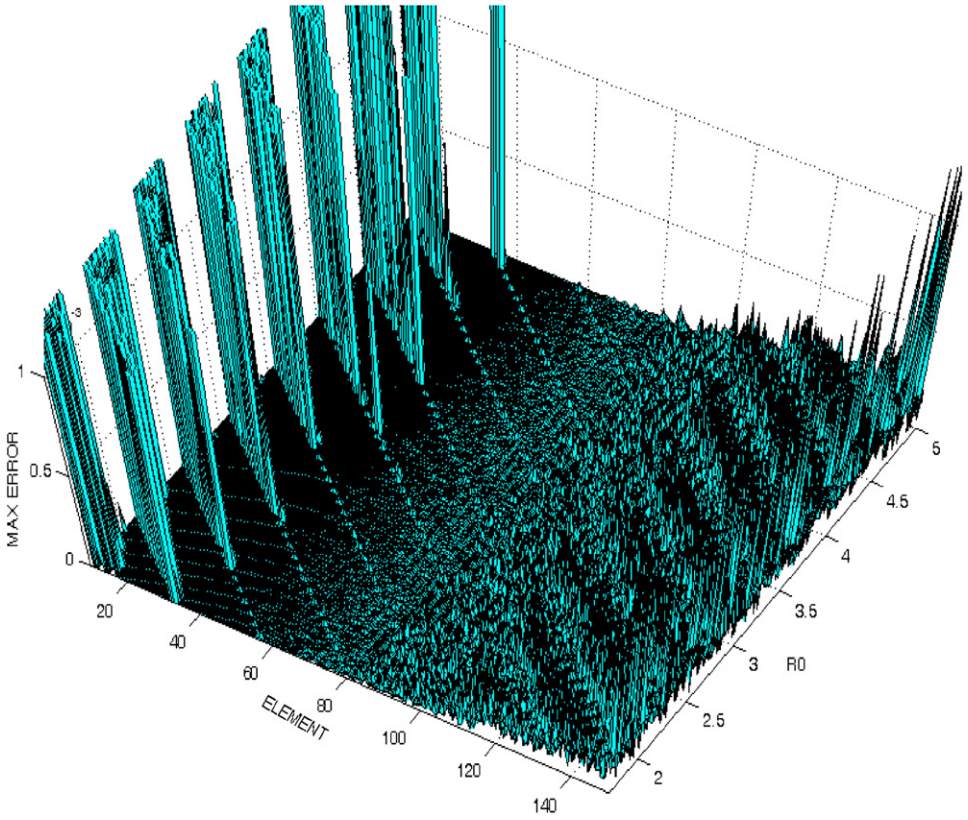

Fig. 7. The distribution of maximum errors under different characteristic lengths and elements.

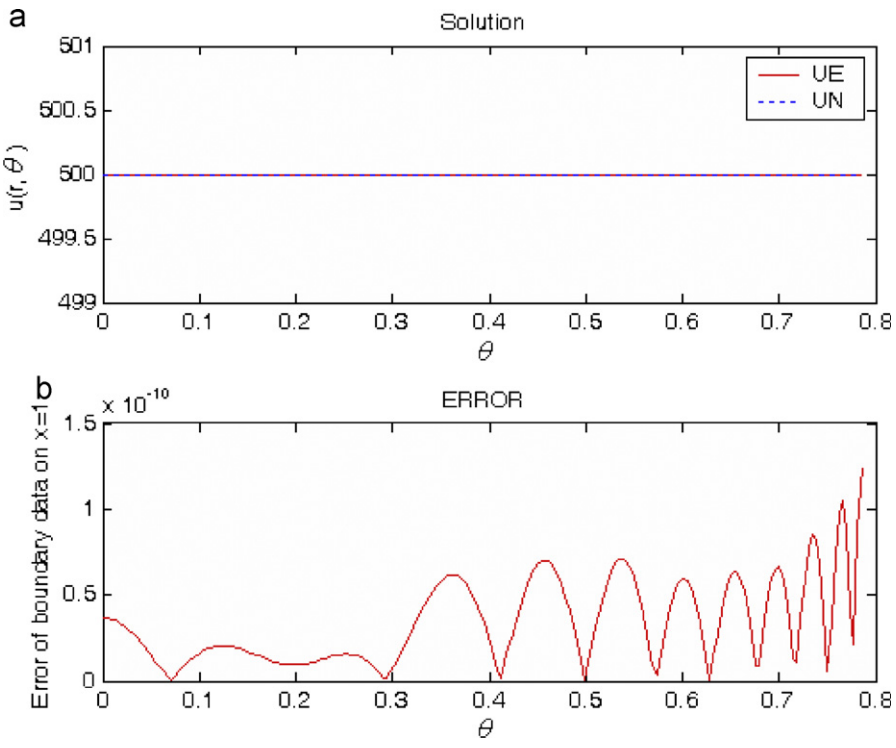

Fig. 8. Comparing the exact solution and numerical solution for Example 3 in (a) and the numerical errors are plotted in (b).

Please cite this article as: Chen Y-W, et al. Applications of the modified Trefftz method for the Laplace equation. Eng Anal Bound Elem (2008), doi:10.1016/j.enganabound.2008.05.008

Hence, we can use the simulated noisy data as the input on our calculations,

$$\widehat{h}(\theta_i) = h(\theta_i) + sR(i), \tag{33}$$

where $\theta_i = 2i\pi/n$, $i = 0,1,\ldots,n$, and s is the level of additive noise on the data. Numerical investigations are carried out to the following examples.

Example 1. This solution domain is a simple two-dimensional disk with radius equal to 2. To illustrate the accuracy and stability of this method we consider the following analytical solution:

$$u(x,y) = \cos x \cosh y + \sin x \sinh y. \tag{34}$$

where $x = 2\cos\theta$ and $y = 2\sin\theta$.

In the numerical computations, we have fixed $\theta_0 = 0$. In Fig. 1, we compare the exact solution with numerical solutions by using different characteristic length and elements (or called numbers of the T-complete function). It can be seen that the maximum errors about 10^{-5} are regular distribution while the geometric shape and boundary conditions are simple. Therefore, we utilize $R_0 = 2.29$ and $m = 30$, and the numerical result and absolute errors are plotted in Fig. 2(a) and (b) with absolute errors smaller than 2×10^{-15}. However, when adding a 5% noise in boundary data, the errors distribution for different characteristic length and elements are shown in Fig. 3. Here, we can find that the trend of the maximum error becomes large when using the T-complete functions from a low order to a high order. Thus, by fixing $R_0 = 98$ and $m = 128$, the numerical solution and exact solution are compared in Fig. 4(a), and the absolute errors are plotted in Fig. 4(b) with absolute errors smaller than 3×10^{-2}. That is to say, when the boundary conditions are contaminated by a large noise, one can control the errors by increasing the characteristic length or elements.

Example 2. For this example, the degenerate scale problem is solved for a thin plate with $a = 20$ and $b = 0.1$. In the inset of Fig. 5, a schematic plot of the plate is shown. We consider the following analytical solution:

$$u(x,y) = x^2 - y^2. \tag{35}$$

In Fig. 5(a), we compare the exact solution with numerical solutions under different characteristic length and elements, and the trend of maximum error is plotted in Fig. 5(a). It can be seen that the maximum error distributes regularly in the region of low-order T-complete functions. We can increase the characteristic length to keep the stability by reducing the degenerate scale effect. By fixing $R_0 = 8214$, we compare the numerical results with $m = 12$ and 112. The numerical result and absolute errors are

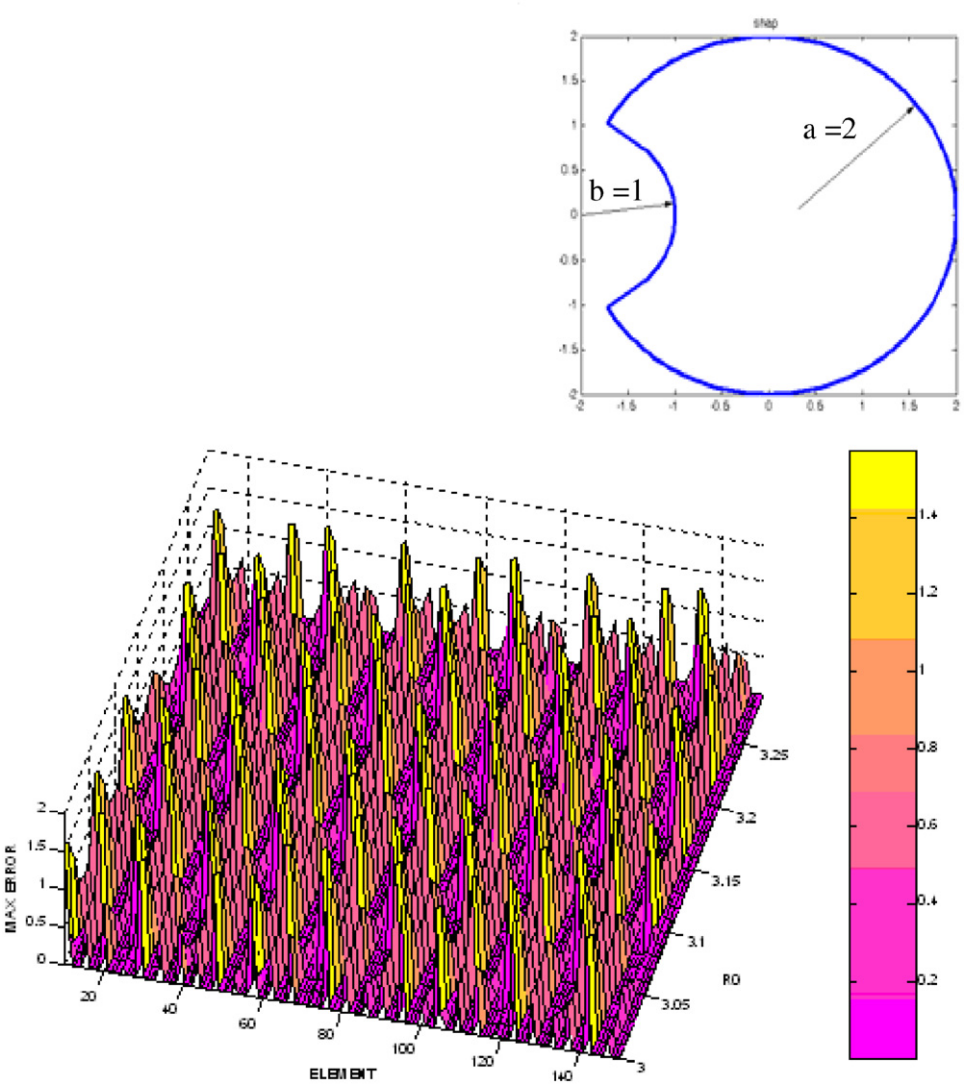

Fig. 9. The distribution of maximum errors under different characteristic lengths and elements.

Please cite this article as: Chen Y-W, et al. Applications of the modified Trefftz method for the Laplace equation. Eng Anal Bound Elem (2008), doi:10.1016/j.enganabound.2008.05.008

shown in Fig. 6(a) and (b). From Figs. 5 and 6, it is clear that the increasing of characteristic length or elements can keep the accuracy and stability, with absolute errors about 4.37×10^{-12} and 1.62×10^{-11}. However, by utilizing the low-order T-complete functions it is easy to make the numerical solution instable, because the range of stability is too narrow to easily choose a suitable characteristic length as shown in Fig. 5.

Example 3. (*Motz problem*). Among the many singular problems, in 1946, Motz first studied the Laplace problem of crack in a narrow rectangular plate, and he found that there was a singularity nearby the tip of crack. Since there is a strong singularity $O(r^{1/2})$ at the original point, the Motz problem has become a benchmark of singularity problem [17], which solves the Laplace equation in a rectangle with length 2 on the horizontal sides and with length 1 on the vertical sides, and the boundary conditions are given by

$$u(1,y) = 500, \quad 0 \leqslant y \leqslant 1, \tag{36}$$

$$u_y(x,1) = 0, \quad -1 \leqslant x \leqslant 1, \tag{37}$$

$$u_x(-1,y) = 0, \quad 0 \leqslant y \leqslant 1, \tag{38}$$

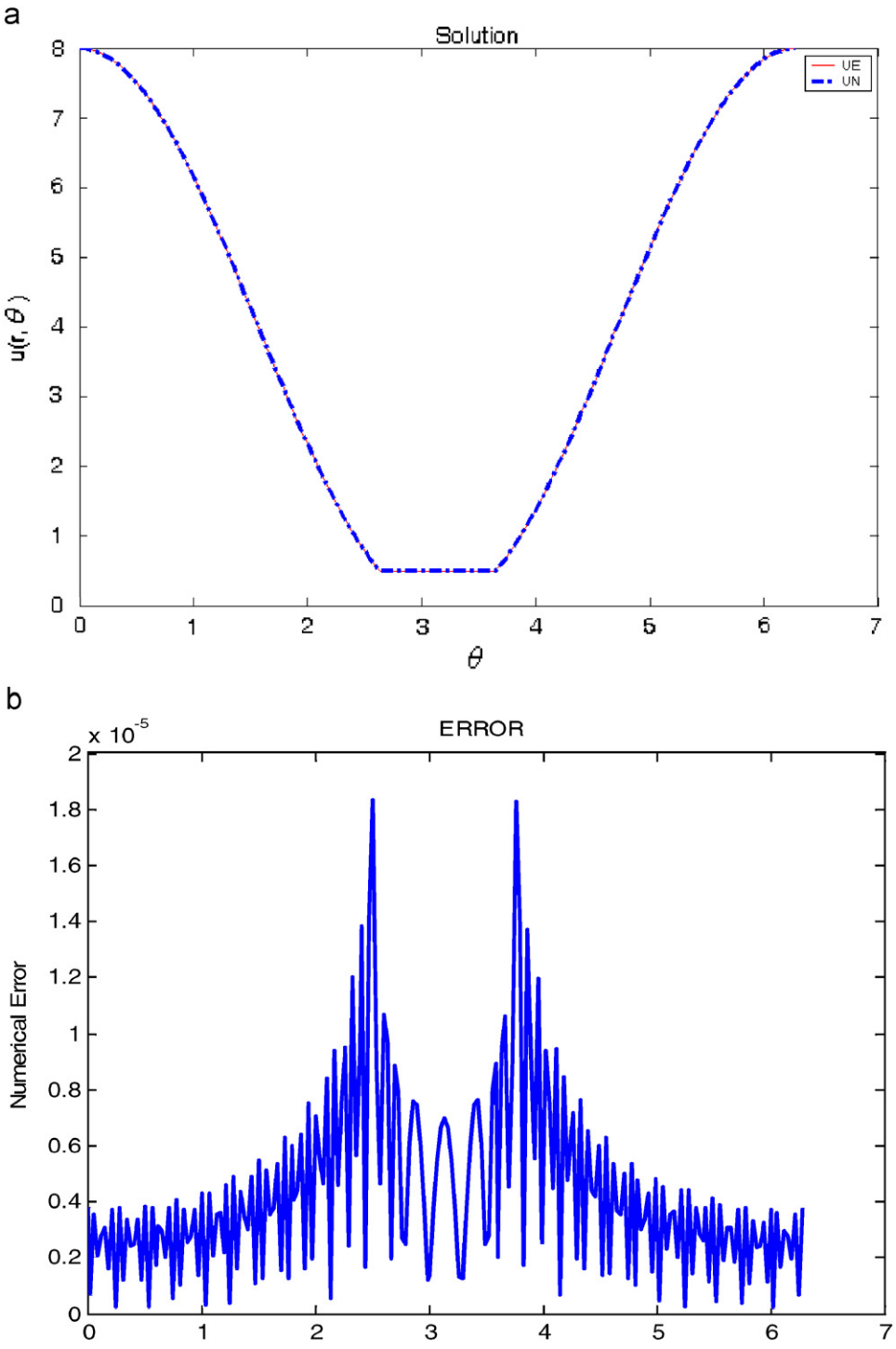

Fig. 10. Comparing the exact solution and numerical solution for Example 4 in (a) and the numerical errors are plotted in (b).

Please cite this article as: Chen Y-W, et al. Applications of the modified Trefftz method for the Laplace equation. Eng Anal Bound Elem (2008), doi:10.1016/j.enganabound.2008.05.008

$$u(x,0)=0, \quad -1\leqslant x<0, \tag{39}$$

$$u_y(x,0)=0, \quad 0\leqslant x\leqslant 1. \tag{40}$$

To solve this problem, the most researchers [18] use the following approximation:

$$u(r,\theta)=\sum_{k=1}^{N} D_k r^{k-(1/2)}\cos\left(k-\frac{1}{2}\right)\theta, \tag{41}$$

which satisfies the Laplace equation and the boundary conditions (39) and (40) automatically. Then the coefficients D_k are determined by the other boundary conditions.

According to Liu [14], we pose a modified approximation given as follows:

$$u(r,\theta)=\sum_{k=1}^{N} C_k\left(\frac{r}{R_0}\right)^{k-(1/2)}\cos\left(k-\frac{1}{2}\right)\theta, \tag{42}$$

where R_0 can be as an extra parameter, which can keep the numerical stability. However, in order to satisfy Eq. (6) for the interior problem, we need to choose $R_0\geqslant\sqrt{2}$.

The maximum numerical error at $x=1$ under different characteristic lengths and elements is shown in Fig. 7. Here, we can find that the use of low-order T-complete functions is extremely easy to cause the numerical solution instability more than the higher order ones when characteristic length and elements are chosen wrong. Liu [14] has obtained the best result with the accuracy about 1.84×10^{-9} when using $N=60$ and $R_0=1.71$. Here, by utilizing $N=232$ and $R_0=1.71$, the numerical result and numerical error of the boundary data at $x=1$ are shown in Fig. 8(a) and (b). Form the numerical result, it can be seen that the maximum error 1.24×10^{-10} is better than that calculated by the low-order T-complete functions.

Example 4. For this example, the torsion problem is considered for a circular shaft with a grove. In the inset of Fig. 9, a schematic plot of the cross section with a grove is shown. We consider the following analytical solution:

$$u(r,\theta)=\frac{b^2}{2}(a^2+ar\cos\theta)\left[1-\frac{ab^2}{r^2+2ar\cos\theta+a^2}\right]. \tag{43}$$

Here, we have expressed the conjugate warping function $u(r,\theta)$ in a polar coordinate with the circular center as the original point. For the most solutions appeared in the literature, the original point is placed at the left-end point of the circle.

The contour shape of this problem is given by

$$\rho(\theta)=\begin{cases}-a\cos-\sqrt{b^2-a^2\sin\theta^2}, & \pi-\phi\leqslant\theta\leqslant\pi+\phi,\\ a & \text{otherwise},\end{cases} \tag{44}$$

where

$$\phi=\arccos\left(\frac{2a^2-b^2}{2a^2}\right). \tag{45}$$

The boundary condition is obtained by inserting Eq. (43) for r into Eq. (42).

In the numerical computations, we have fixed $a=2$, $b=1$ and $\theta_0=0$. In Fig. 10, we compare the exact solution with numerical solutions under different characteristic lengths and elements. It can be seen that maximum errors change extremely acute under different characteristic lengths and elements. Therefore, by fixing $R_0=3.14$ and $m=139$, we compare exact solution with numerical solutions and plot the absolute error in Fig. 10(a) and (b). It can be seen that the numerical solution is close to the exact solution, of which the L^2 error is about 1.83×10^{-5}, better than 8.22×10^{-3} for the low-order T-complete functions of the collocation method and 5.27×10^{-3} for the Galerkin method in literature [13].

5. Conclusions

In this paper, we have applied the modified Trefftz method to calculate the solutions of Laplace problems in arbitrary plane domains. Due to the inclusion of characteristic length to keep the property of high accuracy and stability, the modified Trefftz method could avoid the numerical instability causing by high-order T-complete functions. However, the idea of utilizing the high-order T-complete functions is greatly different from the conventional Trefftz method and other BEM. About this, no matter the geometric shape has discontinuity or singularity of the boundary, the numerical examples show that the stability and the accuracy are very good while utilizing high-order T-complete functions. Therefore, this new method has several advantages than the conventional boundary-type solution method, including meshfree, singularity-free, semi-analyticity, highly accuracy and stability.

Acknowledgement

The corresponding author would like to express his thanks to the National Science Council, Taiwan for their financial supports under contract numbers: NSC-94-2611-E-019-020 and NSC-95-2221-E019-076.

References

[1] Young DL, Chen KH, Lee CW. Novel meshless method for solving the potential problems with arbitrary domain. J Comput Phys 2005;209:290–321.
[2] Chen JT, Shen WC, Chen PY. Analysis of circular torsion bar with circular holes using null-field approach. Comput Model Eng Sci 2006;12:109–19.
[3] Atluri SN, Kim HG, Cho JY. A critical assessment of the truly meshless local Petrov–Galerkin (MLPG), and local boundary integral equation (LBIE) methods. Comput Mech 1999;24:348–72.
[4] Atluri SN, Shen S. The meshless local Petrov–Galerkin (MLPG) method: a simple and less-costly alternative to the finite element and boundary element methods. Comput Model Eng Sci 2002;3:11–51.
[5] Trefftz E. Ein Gegenstück zum Ritzschen Verfahren. In: Proceedings of the second international congress on applied mechanics, Zurich, 1926. p. 131–7.
[6] Herrera I. Theory of connectivity: a systematic formulation of boundary element methods. In: Brebbia CA, editor. New developments in boundary element methods (Proceedings of the second international seminar on recent advances in BEM, Southampton, England, 1980). Plymouth: Pentech Press; 1980. p. 45–58.
[7] Kita E, Ikoda Y, Kamiya N. Indirect Trefftz method for boundary value problem of Poisson equation. Eng Anal Bound Elem 2003;27:825–33.
[8] Berardi SC, Berardi SR. The Trefftz boundary method in viscoelasticity. Comput Model Eng Sci 2005;29:383–90.
[9] Kita E, Katsuragawa J, Kamiya N. Application of Trefftz-type boundary element method to simulation of two-dimensional sloshing phenomenon. Eng Anal Bound Elem 2004;28:677–83.
[10] Lu TT, Hu HY, Li ZC. Highly accurate solutions of Motz's and the cracked beam problems. Eng Anal Bound Elem 2004;28:1387–403.
[11] Portela A, Charafi A. Trefftz boundary element: multi-region formulations. Int J Numer Meth Eng 1999;45(7):821–46.
[12] Li ZC, Lu TT, Huang HT, Cheng AHD. Trefftz, collocation, and other boundary methods—a comparison. Numer Meth Part Diff Eq 2007;23:93–144.
[13] Liu CS. An effectively modified direct Trefftz method for 2D potential problems considering the domain's characteristic length. Eng Anal Bound Elem 2007;31:983–93.
[14] Liu CS. A highly accurate solver for the mixed-boundary potential problem and singular problem in arbitrary plane domain. Comput Model Eng Sci 2007; 20(2):111–22.
[15] Liu CS. A modified Trefftz method for two-dimensional Laplace equation considering the domain's characteristic length. Comput Model Eng Sci 2007; 21(1):53–65.
[16] Liu CS. A meshless regularized integral equation method for Laplace equation in arbitrary interior or exterior plane domains. Comput Model Eng Sci 2007;19(1):99–109.
[17] Li ZC. Combined methods for elliptic equations with singularities, interfaces and infinities. Netherlands: Kluwer Academic Publishers; 1998.
[18] Lu TT, Hu HY, Li ZC. Highly accurate solutions of Motz's and the cracked beam problems. Eng Anal Bound Elem 2004;28:1387–403.

Please cite this article as: Chen Y-W, et al. Applications of the modified Trefftz method for the Laplace equation. Eng Anal Bound Elem (2008), doi:10.1016/j.enganabound.2008.05.008